Non-isothermal compositional liquid gas Darcy flow: formulation and soil-atmosphere boundary condition applied to high energy geothermal simulations.

Laurence Beaude

Supervisors:

Roland MASSON
Konstantin BRENNER
Simon LOPEZ
Farid SMAI

2017-11-13

Introduction

Goal: study the model and the formulation of compositional gas liquid Darcy flow and include an advanced boundary condition at the interface between the porous medium and the atmosphere accounting for convective mass and energy transfer, liquid evaporation and liquid outflow.

Main points:

- non-isothermal compositional gas liquid Darcy flow model,
- geothermal activity close to the surface: necessity to **model of a soil-atmosphere boundary condition**

The study is applied on the high energy geothermal field Bouillante in Guadeloupe.

Introduction

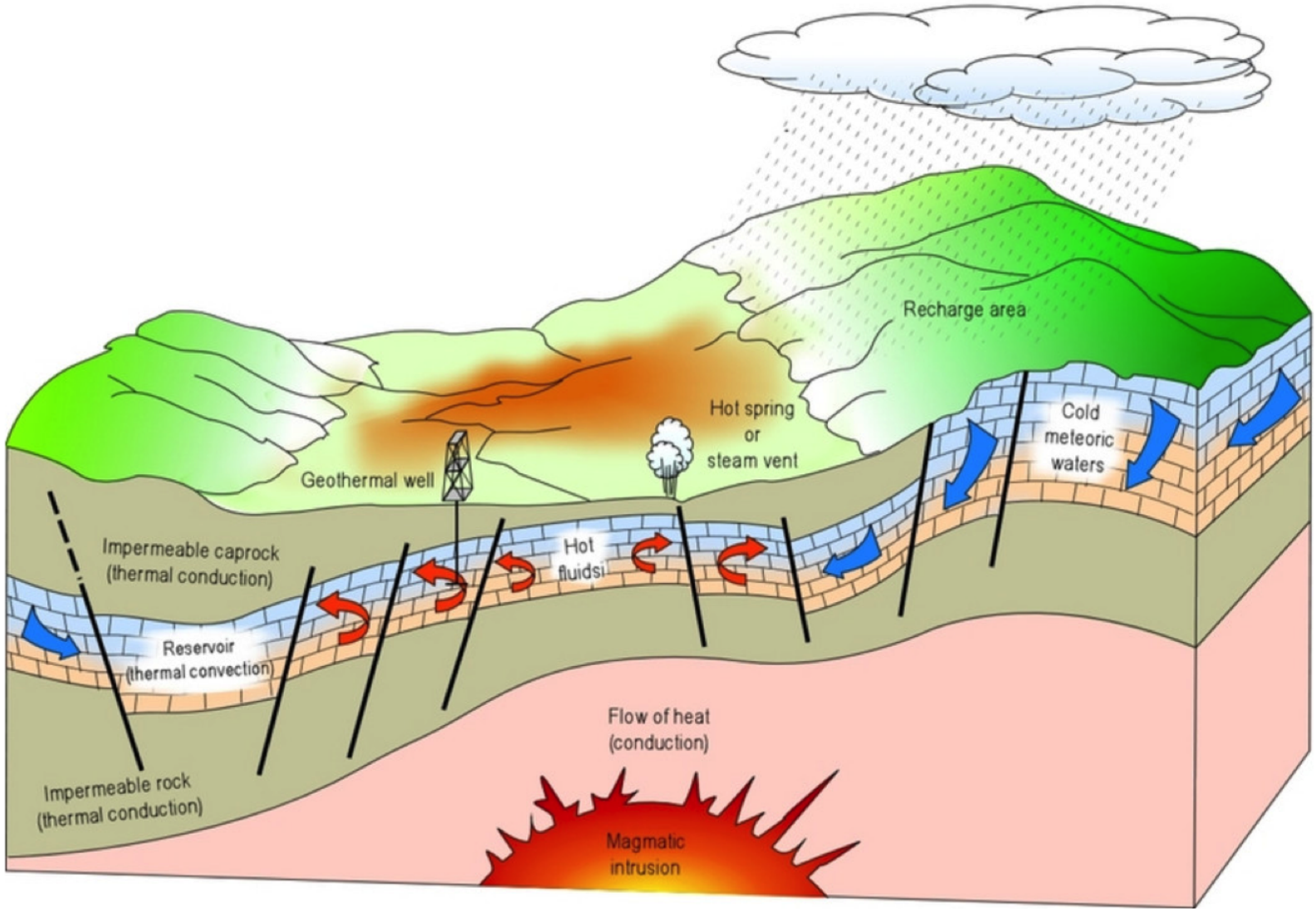

Figure: High energy geothermal field.

Layout

1. Model
   - Porous medium model
   - Soil-atmosphere boundary condition
2. Discretization and non-linear solvers
3. Test cases
   - Validation of the soil-atmosphere evaporation boundary condition
   - 2D geothermal test cases
4. Perspectives

Layout

Single phase Darcy flow

$$\begin{cases} \text{Darcy law:} & \mathbf{V} = -\frac{\mathbf{\Lambda(x)}}{\mu}\Big(\nabla P - \rho(P)\mathbf{g}\Big), \\ \text{molar conservation:} & \phi\partial_t\zeta(P) + \operatorname{div}(\zeta(P)\mathbf{V}) = 0. \end{cases}$$

P: pressure (Pa)
$\mathbf{V}$: Darcy velocity $(\mathrm{m.s^{-1}})$
$\mathbf{\Lambda(x)}$:permeability tensor of the porous medium $(\mathrm{m^2})$
ϕ: porosity of the porous medium
μ: viscosity of the fluid $(\mathrm{Pa.s})$
ζ: molar density of the fluid $(\mathrm{mol.m^{-3}})$
ρ: mass density of the fluid $(\mathrm{kg.m^{-3}})$

Two phase Darcy velocities

$$\begin{cases} \mathbf{V}^\alpha = -\frac{k_r^\alpha(S^\alpha)}{\mu^\alpha}\mathbf{\Lambda}(\mathbf{x})\Big(\nabla P^\alpha - \rho^\alpha \mathbf{g}\Big), \\ P^g - P^l = P_c(S^g), \\ S^g + S^l = 1. \end{cases}$$

$\alpha = g, l$: phases
S^α: volume fractions
P^α: pressures
P_c: capillary pressure (in Pa)

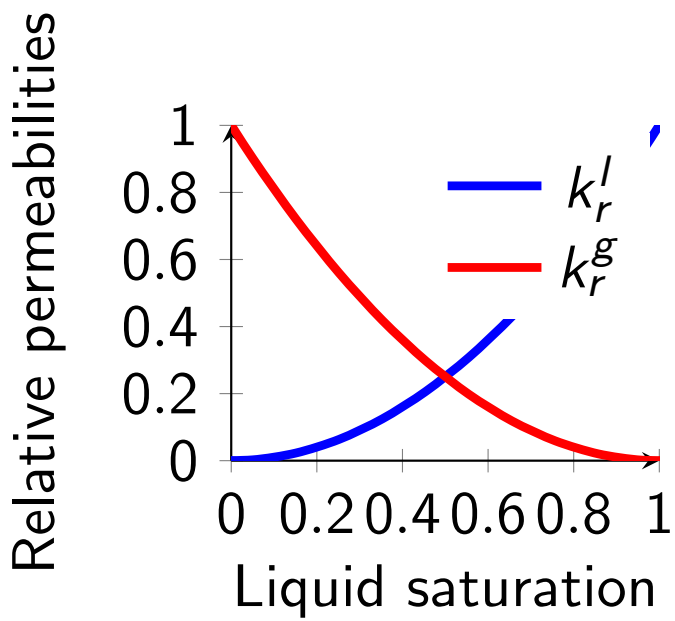

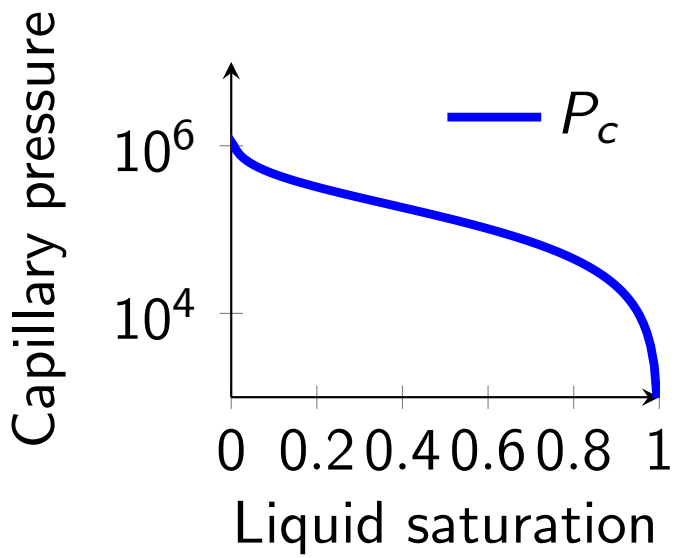

Non-isothermal compositional liquid-gas Darcy equations

Molar conservation of each component $i \in \mathcal{C}$, typically $\mathcal{C} = \{\text{water}, \text{air}\}$

$$\phi \partial_t n_i + \operatorname{div}\Big(\sum_{\alpha=g,l} \zeta^\alpha c_i^\alpha \mathbf{V}^\alpha \Big) = 0, \quad i \in \mathcal{C},$$

together with the energy conservation

$$\partial_t \Big(\phi \sum_{\alpha=g,l} \zeta^\alpha e^\alpha S^\alpha + (1-\phi) e_r \Big) + \operatorname{div}\Big(\sum_{\alpha=g,l} \zeta^\alpha h^\alpha \mathbf{V}^\alpha \Big) + \operatorname{div}(-\lambda \nabla T) = 0$$

complemented by local closure laws $P^g - P^l = P_c(S^g)$ and $S^g + S^l = 1$ and the **thermodynamic equilibrium**.

$c^\alpha = (c_i^\alpha)_{i \in \mathcal{C}}$: molar fractions
$n_i = \sum_{\alpha \in \mathcal{P}} \zeta^\alpha \ S^\alpha \ c_i^\alpha$: number of moles per unit pore volume
e^α: molar internal energy, h^α: molar enthalpy, λ: thermal conductivity

Two families of formulations

The formulations differ by their choice of the unknowns and equations and by the way they deal with phase transitions (in non-isothermal models, the **thermodynamic equilibrium states for the present phases**).

- **Variable switch formulations:** adapt the set of principal unknowns and equations to the set of present phases which can vary in space and time (eg. Coats' formulation).
- **Persistent variable formulations:** based either on natural physical quantities or on non-standard principal variables. Another strategy to avoid the switch of variables is based on the extension of some physical quantities.

Specificity of our formulation

Our formulation of the model leads to the fix sets of $2\#\mathcal{C} + 5$ unknowns

$$X = \Big(P^\alpha, T, S^\alpha, c^\alpha, \alpha = g, l\Big),$$

All the physical laws are directly expressed using subsets of this set of variables. It is also a convenient in single phase regions. To avoid the switch of variables, we extend the phase molar fractions of an absent phase by the molar fractions at thermodynamic equilibrium with the present phase.

Also the thermodynamic equilibrium is expressed as **complementary constraints** which allow the use of **semi-smooth Newton methods** to solve the non-linear system at each time step of the simulation

$$\begin{cases} S^\alpha \geq 0,\ 1 - \sum_{i \in \mathcal{C}} c_i^\alpha \geq 0,\ S^\alpha (1 - \sum_{i \in \mathcal{C}} c_i^\alpha) = 0, & \alpha = g, l, \\ f_i^g(P^g, T, c^g) = f_i^l(P^l, T, c^l), & i \in \mathcal{C}. \end{cases}$$

Layout

Motivations

The geothermal activity of the Bouillante field is characterized by a high temperature close to the surface (the temperature reaches 250 °C at 300m deap and approaches 100 °C at the surface). And the coupling between the porous medium and surface flows is not computationally realistic at the space and time scales of a geothermal flow, then our objective is rather to model the soil-atmosphere interaction using an advanced boundary condition.

BC: vaporization and liquid outflow

The soil-atmosphere interaction is based on **mole and energy balance equations set at the interface**. Convective molar and energy transfer in the atmosphere states the **continuity of the component molar and energy normal fluxes**, assuming instantaneous vaporization of the liquid phase, as well as the **continuity of the gas phase** (c^g, T and P^g).

At the interface is introduced two additional unknowns:

- $q^{g,atm}$ the gas molar flow rate,
- $q^{l,atm}$ the liquid molar flow rate (liquid outflow),

both unknowns are expressed at the interface on the atmosphere side oriented positively outward from the porous-medium domain.

The far field atmospheric conditions $c_\infty^{g,atm}$, T_∞^{atm} and P^{atm} are imposed.

Fluxes balance at the interface

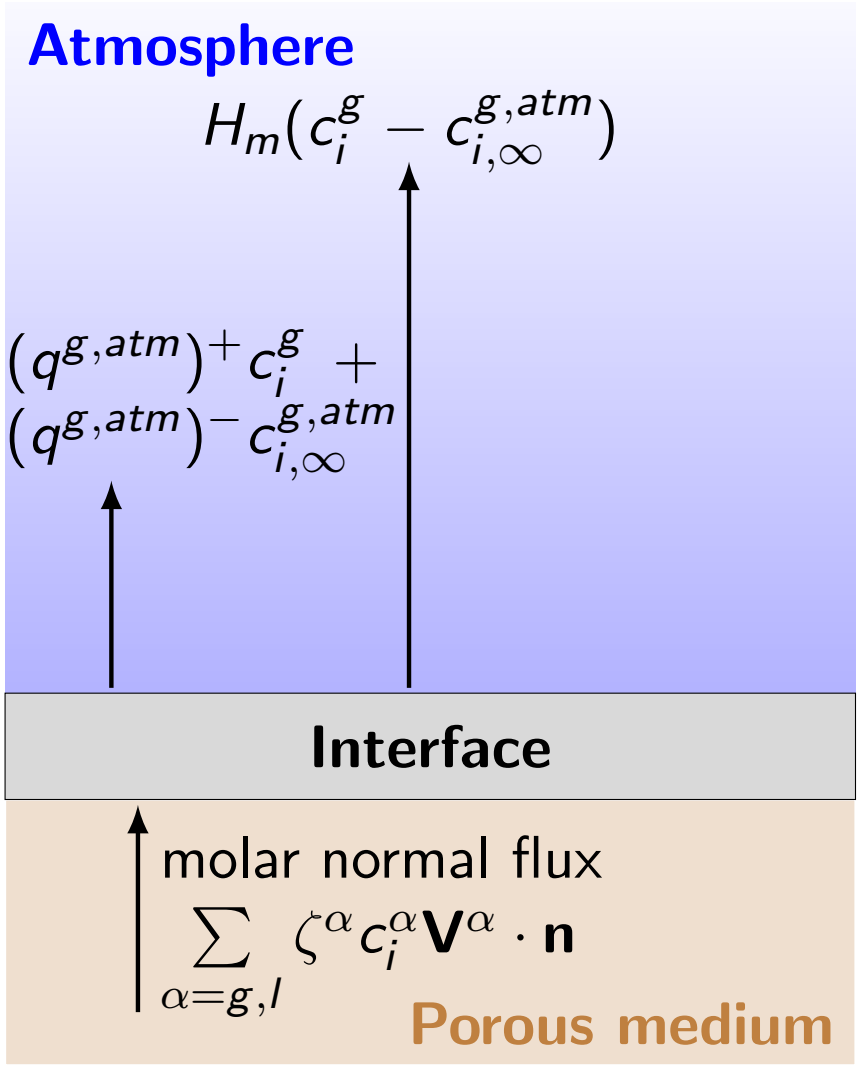

Figure: Molar fluxes balance.

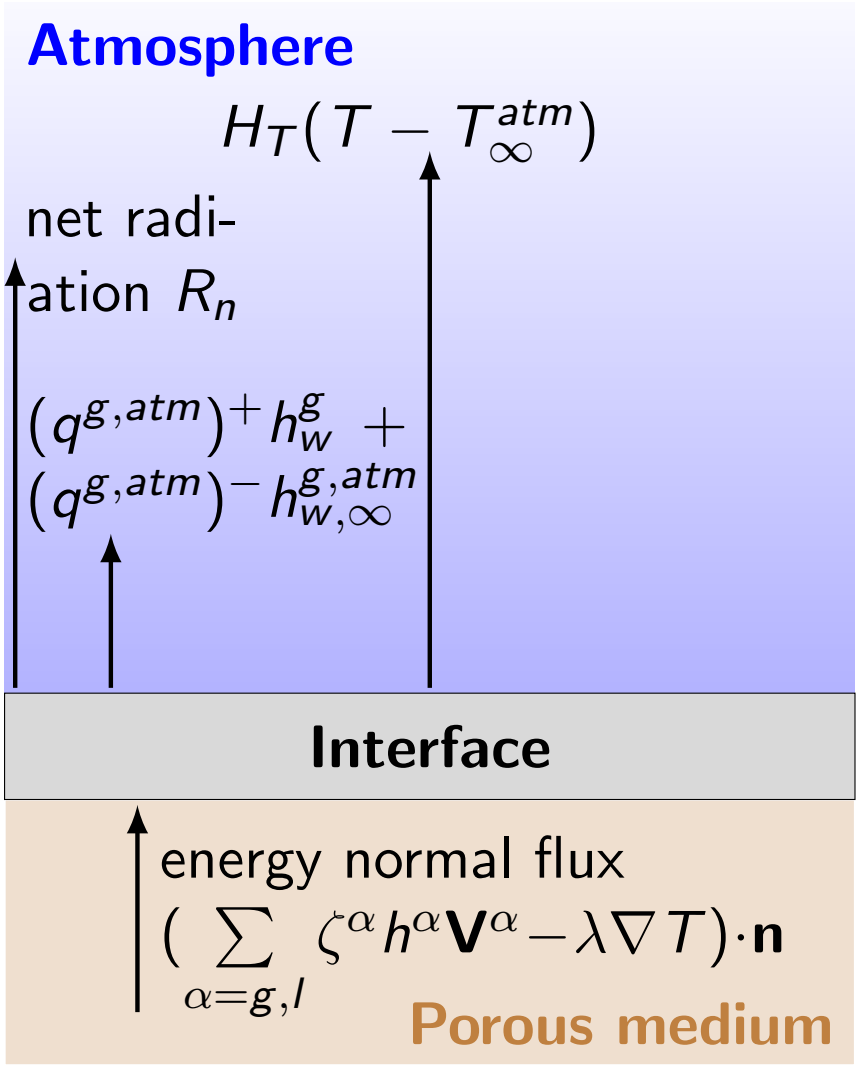

Figure: Energy fluxes balance.

Fluxes balance at the interface

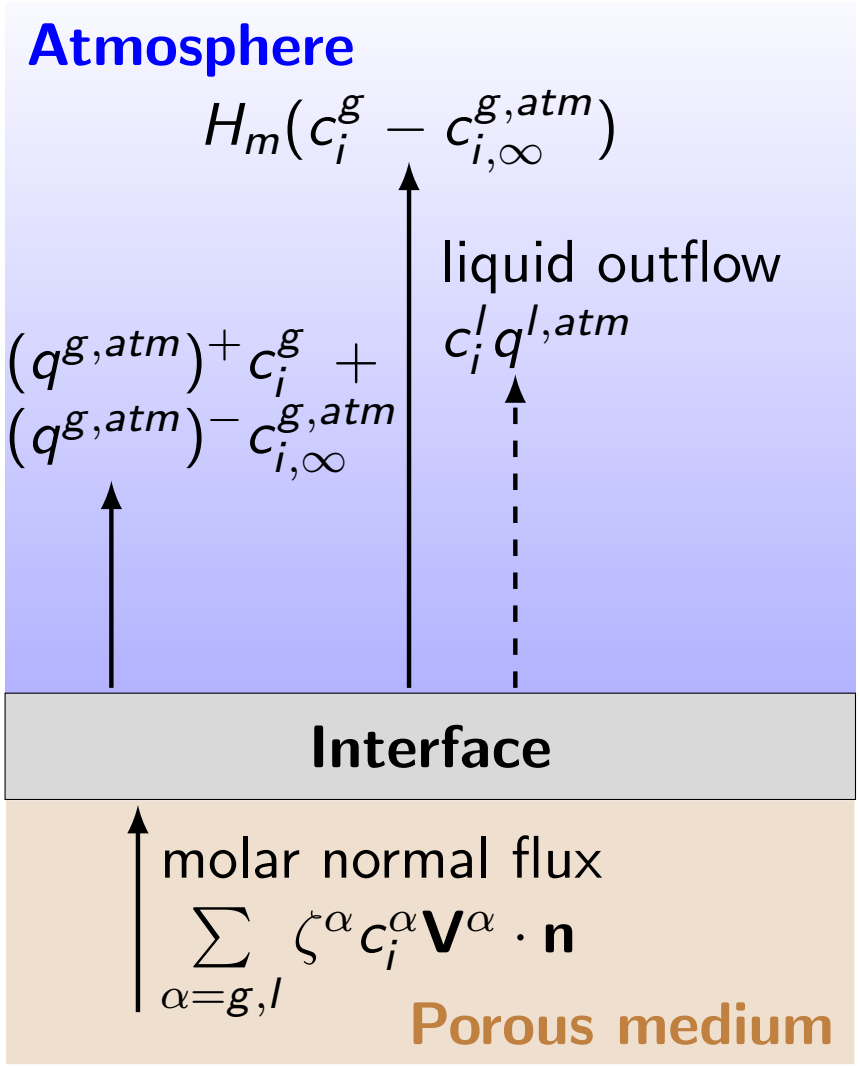

Figure: Molar fluxes balance.

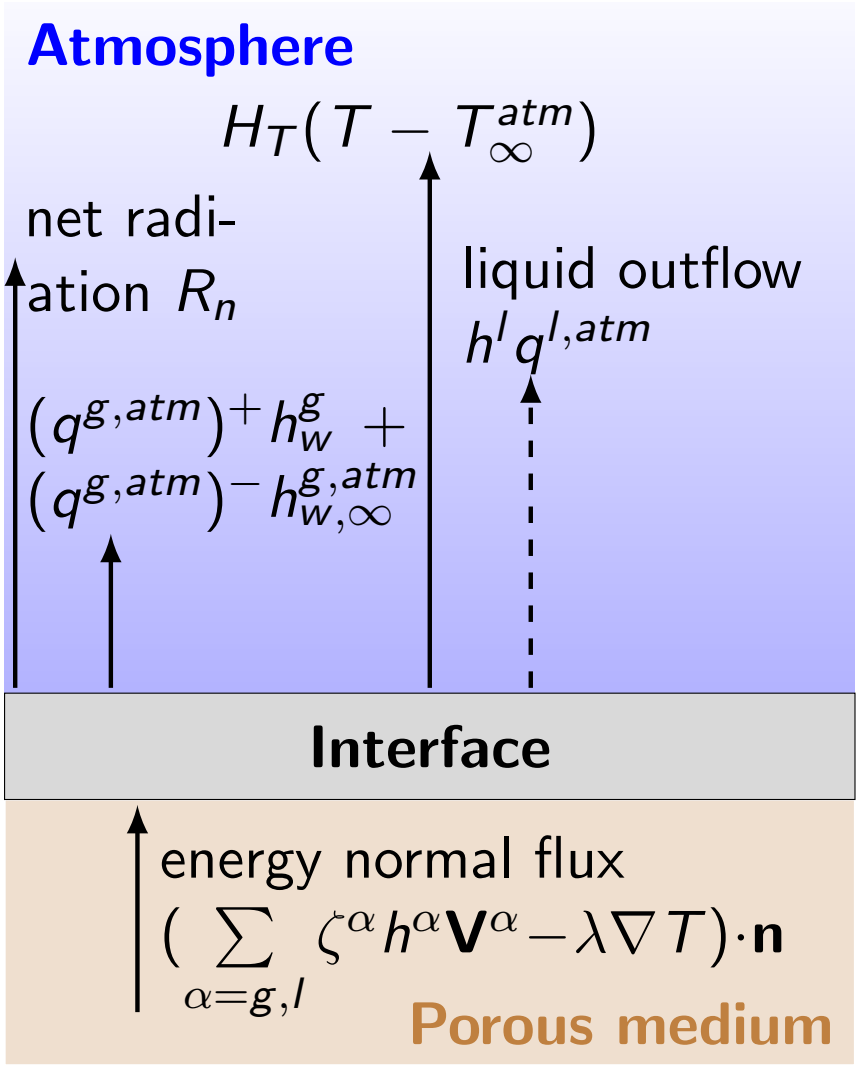

Figure: Energy fluxes balance.

Fluxes balance at the interface

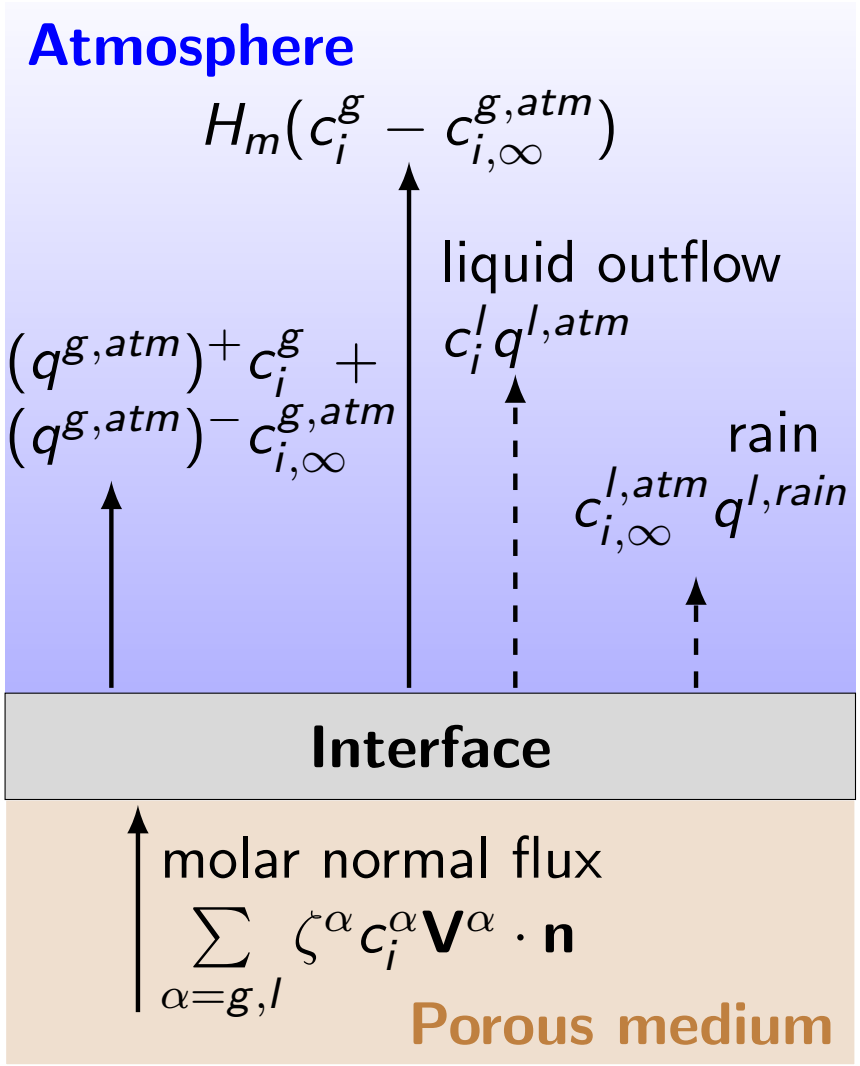

Figure: Molar fluxes balance.

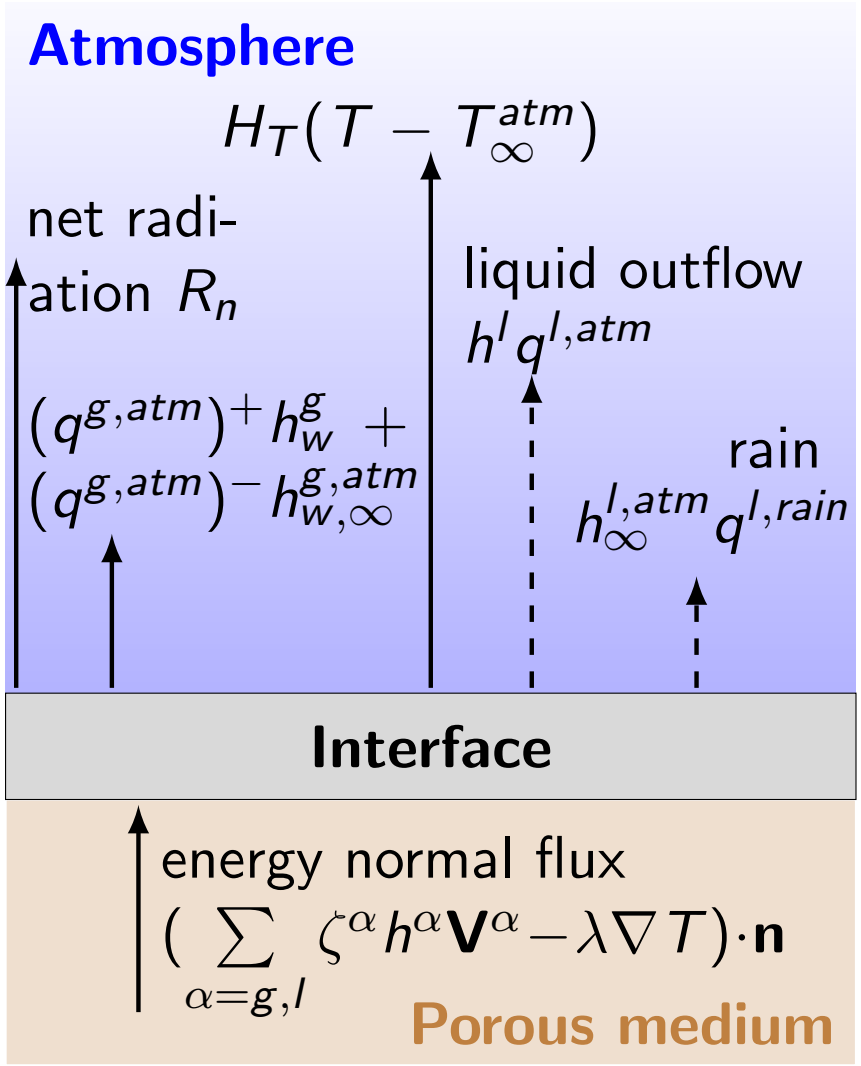

Figure: Energy fluxes balance.

Liquid outflow complementary constraints

Which constraints on the liquid outflow $q^{l,atm}$?

Let us denote by $c^{l,atm}$ the liquid molar fraction at the interface on the atmosphere side. The liquid outflow condition writes:

$$\begin{cases} (1 - \sum_{i \in \mathcal{C}} c_i^{l,atm}) q^{l,atm} = 0, \\ 1 - \sum_{i \in \mathcal{C}} c_i^{l,atm} \geq 0, \; q^{l,atm} \geq 0, \end{cases}$$

Thanks to the thermodynamic equilibrium and the continuity of the gas phase at the interface, the liquid outflow complementary constraint is equivalent to:

$$\begin{cases} (P^g - P^l) q^{l,atm} = 0, \\ P^g - P^l \geq 0, \; q^{l,atm} \geq 0, \end{cases}$$

Soil-atmosphere boundary condition

The system becomes:

$$\begin{aligned}
\mathbf{V}_i \cdot \mathbf{n} &= (q^{g,atm})^+ c_i^g + (q^{g,atm})^- c_{i,\infty}^{g,atm} + H_m \left(c_i^g - c_{i,\infty}^{g,atm} \right) \\
&\quad + c_i^l q^{l,atm} + c_{i,\infty}^{l,atm} q^{l,rain}, \quad i \in \mathcal{C}, \\
\mathbf{V}_e \cdot \mathbf{n} &= (q^{g,atm})^+ h_w^g(P^g, T, c^g) + (q^{g,atm})^- h_{w,\infty}^{g,atm} + H_T(T - T_\infty^{atm}) \\
&\quad + h^l(P^l, T, c^l) q^{l,atm} + (1-a) R_s + R_a - \epsilon \sigma T^4 + h_\infty^{l,atm} q^{l,rain}.
\end{aligned}$$

+ local closure laws

And the $2\#\mathcal{C} + 7$ unknowns are:

$$X = \left(q^{g,atm}, q^{l,atm}, P^\alpha, T, S^\alpha, c^\alpha, \alpha = g, l \right),$$

BC local closure laws

$$
\begin{cases}
P^g = P^{atm}, \\
S^g = \mathcal{S}^g(P^g - P^l), \\
S^g + S^l = 1, \\
\sum_{i \in \mathcal{C}} c_i^g = 1, \\
S^l \geq 0,\ 1 - \sum_{i \in \mathcal{C}} c_i^l \geq 0,\ S^l(1 - \sum_{i \in \mathcal{C}} c_i^l) = 0, \\
f_i^g(P^g, T, c^g) = f_i^l(P^l, T, c^l),\ \ i \in \mathcal{C} \\
P^g - P^l \geq 0,\ q^{l,atm} \geq 0,\ (P^g - P^l) q^{l,atm} = 0.
\end{cases}
$$

Layout

Discretization

- Fully implicit Euler scheme
- Finite volume in space with a TPFA of the Darcy and Fourier fluxes
- Phase based upwind scheme for the approximation of the mobilities, molar fractions and enthalpies.
- Admissibility condition of TPFA schemes (we chose Voronoi mesh with isotropic permeability)
- **Newton-min non-linear solver**

To reduce the size of the linear systems to be solved at each Newton-min iteration to $\#\mathcal{C}+1$ equations and unknowns, the set of unknowns is splitted into $\#\mathcal{C}+1$ primary unknowns and the remaining secondary unknowns. The splitting is done for each degree of freedom and depends on the present phases.

Newton-min non-linear solver

- **basic version**: at each Newton iterate enforces only $P^g - P^l = P_c(S^g)$. Also needs to project $c^\alpha \in [-0.2; 1.2]$.
- **Newton-min with projection on the complementary constraints**: at each Newton iterate all the complementary constraints are enforced, $P^g - P^l = P_c(S^g)$ is imposed as well as the physical ranges:

$$\left\{ \begin{array}{l} \min\left(S^\alpha, 1 - \sum_{i \in \mathcal{C}} c_i^\alpha\right) = 0, \\ \text{if } S^\alpha > 0 \text{ then } 0 \leq c_i^\alpha \leq 1, \quad i \in \mathcal{C}, \quad \alpha = g, l, \\ S^\alpha \geqslant 0, \quad \alpha \in \mathcal{P}, \quad \sum_{\alpha = g,l} S^\alpha = 1. \end{array} \right.$$

- **Newton-min with projection on the complementary constraints and thermodynamic equilibrium**: in addition to the previous updates, the molar fractions which are secondary unknowns, plus the temperature if both phases are present, are updated in order to verify:

$$f_i^g(P^g, T, c^g) = f_i^l(P^l, T, c^l), \quad i \in \mathcal{C}$$

Layout

Comparison to a full-dimensional free-flow model

The full-dimensional free-flow model is a non-isothermal compositional Reynold Average Navier-Stokes (RANS) gas flow. The coupling conditions at the interface assume the vaporization of the liquid phase in the free-flow domain, the gas molar fraction and molar and energy normal flux continuity, the liquid gas thermodynamic equilibrium, the no slip condition and the normal component of the normal stress continuity.

Domains of the two models

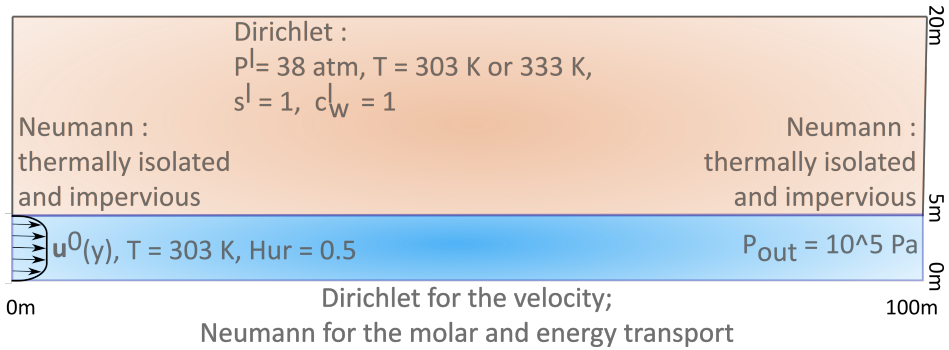

Figure: Computational domain of the coupled Darcy and full-dimensional free-flow models.

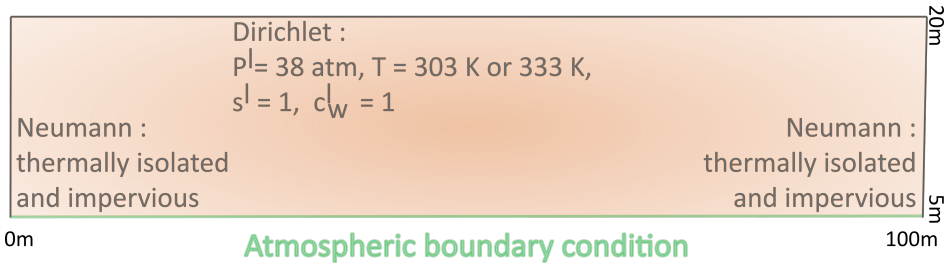

Figure: Computational domain of the Darcy flow model coupled with the soil-atmosphere evaporation-outflow boundary condition.

Comparison to a full-dimensional free-flow model with $T^0_{pm} = 303\ \mathrm{K}$

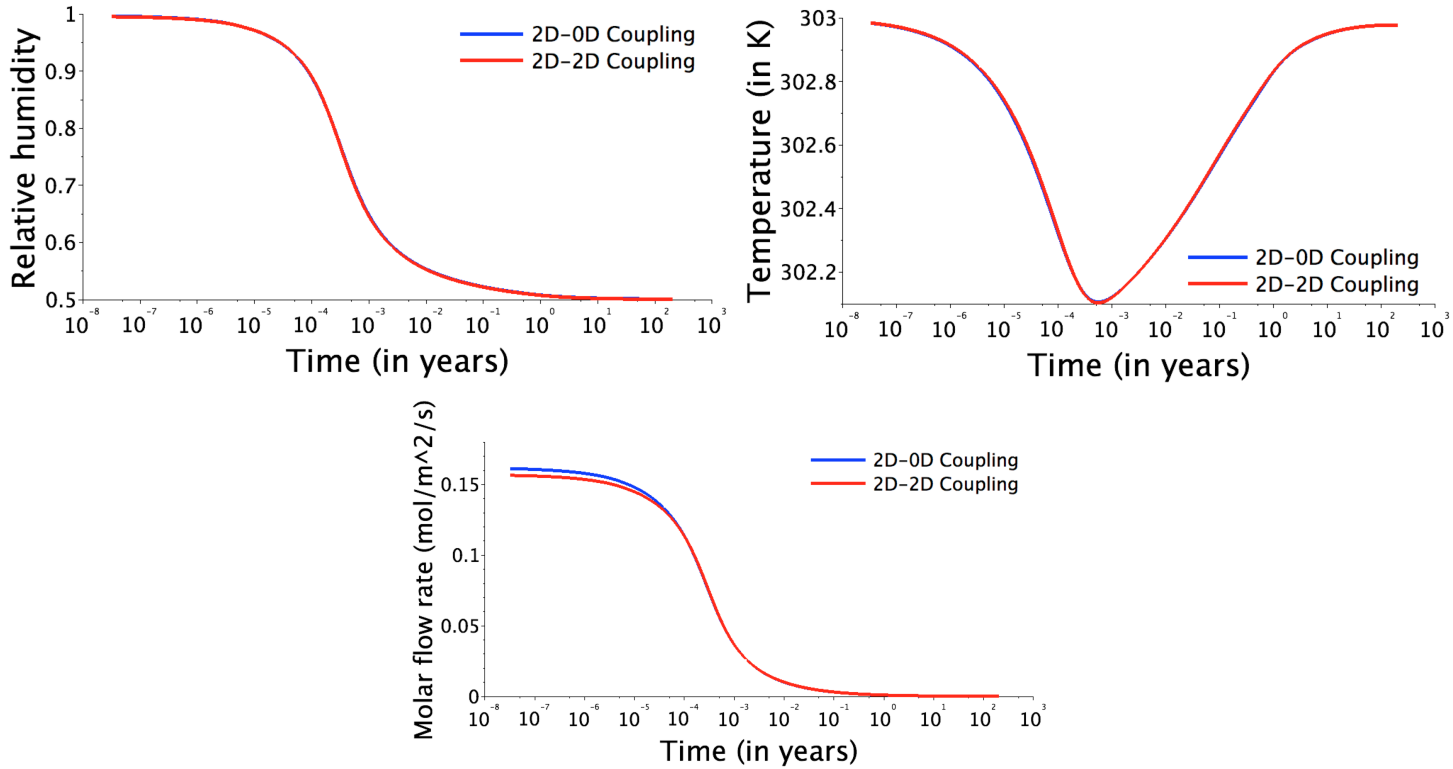

Figure: Mean relative humidity, mean temperature (in K) and molar flow rate of the water component (in $\mathrm{mol.m^{-2}.s^{-1}}$) at the interface as a function of time (in years) for both models with $T^0_{pm} = 303\ \mathrm{K}$.

Comparison to a full-dimensional free-flow model with $T^0_{pm} = 333\ \mathrm{K}$

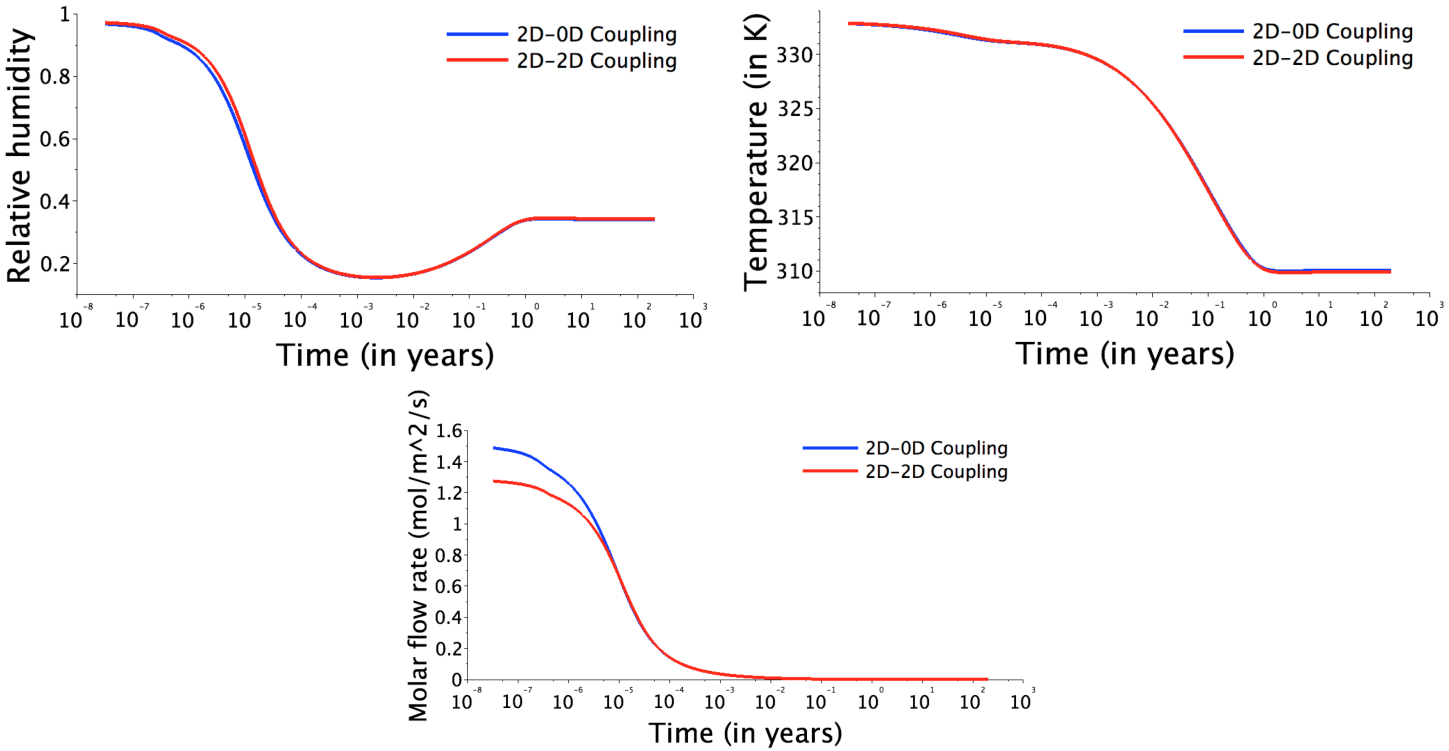

Figure: Mean relative humidity, mean temperature (in K) and molar flow rate of the water component (in $\mathrm{mol.m^{-2}.s^{-1}}$) at the interface as a function of time (in years) for both models with $T^0_{pm} = 333\ \mathrm{K}$.

Numerical efficiency of the Newton-min non-linear solvers

$N_x \times N_y$	100×60	100×90
Basic Newton-min	$\times$	$\times$
Newton-min with projection	157/0/613/497	182/2/886/1360
Newton-min with projection and thermodynamic equilibrium	157/0/586/523	157/0/612/972

Table: Number of time steps, of time step chops, total number of Newton iterations and CPU time for the three Newton-min methods obtained with $N_y = 60, 90$ and $T^0_{pm} = 333\ \mathrm{K}$.

BC setting of the 2D geothermal test cases

Impact of the advanced soil-atmosphere boundary condition.

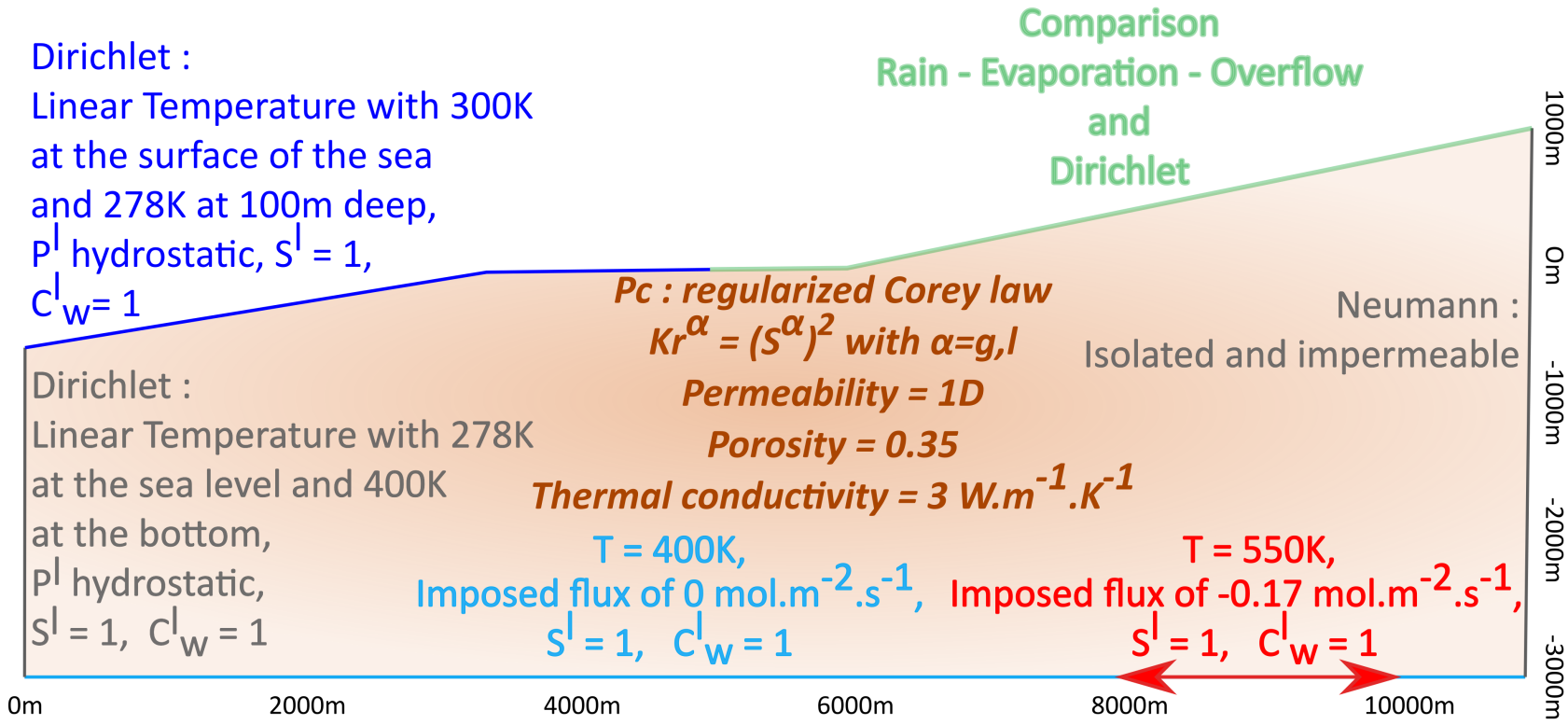

Figure: Illustration of the Bouillante domain and boundary conditions of the geothermal test cases.

BC parameters at the upper boundary

Evaporation-outflow BC ($0 < z$): $(1-a)R_s + R_a = 340\ W/m^2$, $\epsilon = 0.97$, $c_{a,\infty}^{g,atm} = 0.99$, $c_{w,\infty}^{g,atm} = 0.01$, $T_\infty^{atm} = 300\ K$, $P^{atm} = 1\ atm$, $H_m = 0.69\ mol/m^2/s$, $H_T = 29 * H_m = 20\ W/m^2/K$.

Precipitation recharge ($500 < z$): $q^{l,rain} = -0.032\ mol/m^2/s$, $c_{w,\infty}^{l,atm} = 0.999$.

Seabed Dir ($z \leq 0$): $S^l = 1$, $c_w^l = 1$, hydrostatic pressure P^l, linear T with $300K$ at the sea level and $278K$ at $100m$ depth.

Sunny plain Dir ($0 < z \leq 500$): $S^g = 1$, $c_a^g = 0.99$, $c_w^g = 0.01$, $P^g = 1\ atm$, $T = 300\ K$.

Rainy zone Dir ($500 < z$): $S^g = 0.72$, $c_a^g = 0.97$, $c_w^g = 0.03$, $c_a^l = 0.001$, $c_w^l = 0.999$, $P^g = 1\ atm$, $T = 300\ K$.

Results: impact of the advanced boundary condition

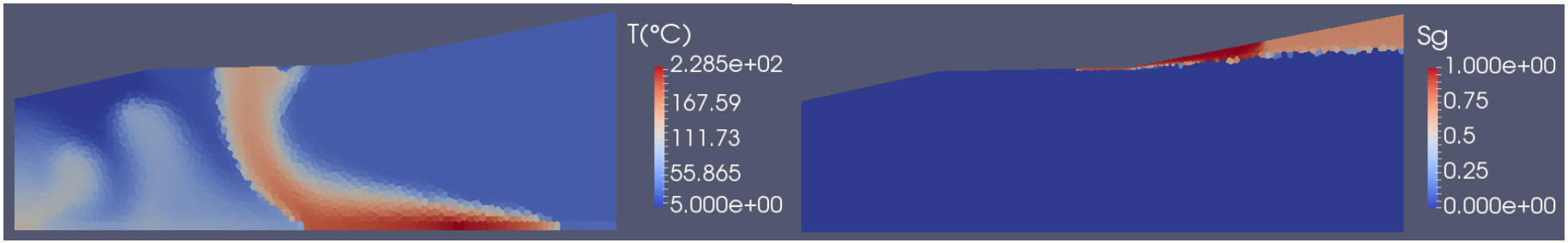

Figure: Temperature (in Celsius) and gas saturation at final time (1000 years) obtained with the Dirichlet top boundary conditions.

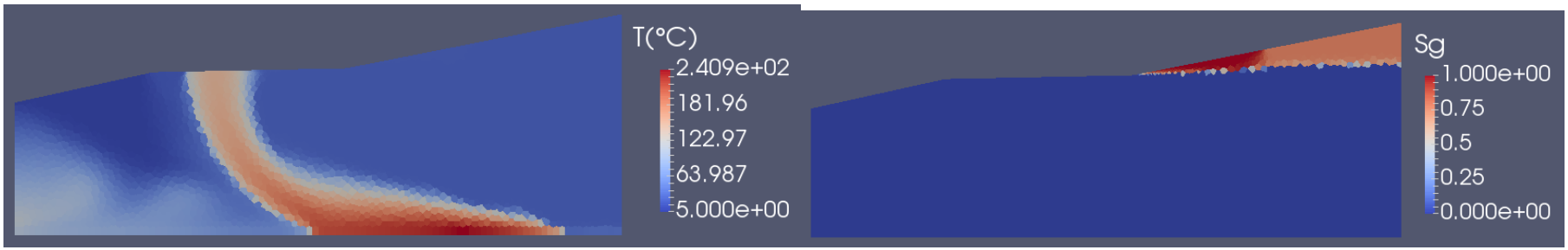

Figure: Temperature (in Celsius) and gas saturation at final time (1000 years) obtained with the evaporation-outflow boundary condition.

The evaporation-outflow boundary condition shifts the high temperature zone to the left. The gas saturation remains null below the seabed and the desaturated zone is shifted to the right and is deeper.

2D geothermal test case with 3 components

Convective thermal instabilities can be noticed which are induced artificially by the left Dirichlet boundary condition. We add salt !
We introduce the salinity C_s in $\mathrm{kg.\,kg^{-1}}$

$$C_s = \frac{c_s^l m_s}{\sum_{i \in \mathcal{C}} c_i^l m_i},$$

with $m_s = 58.44 \cdot 10^{-3}$, $m_w = 18 \cdot 10^{-3}$, $m_a = 29 \cdot 10^{-3}$ $\mathrm{kg.\,mol^{-1}}$.
The seabed Dirichlet BC now uses the input salinity $C_s = 35 \cdot 10^{-3}$ $\mathrm{kg.\,kg^{-1}}$ of the sea water. The input salinity at the left side of the reservoir as well as at the bottom boundary is fixed to $C_s = 20 \cdot 10^{-3}$ $\mathrm{kg.\,kg^{-1}}$.

Since our model assumes all components to be present in both phases, the liquid and gas phases are now a mixture of three components.

Results: impact of the salt

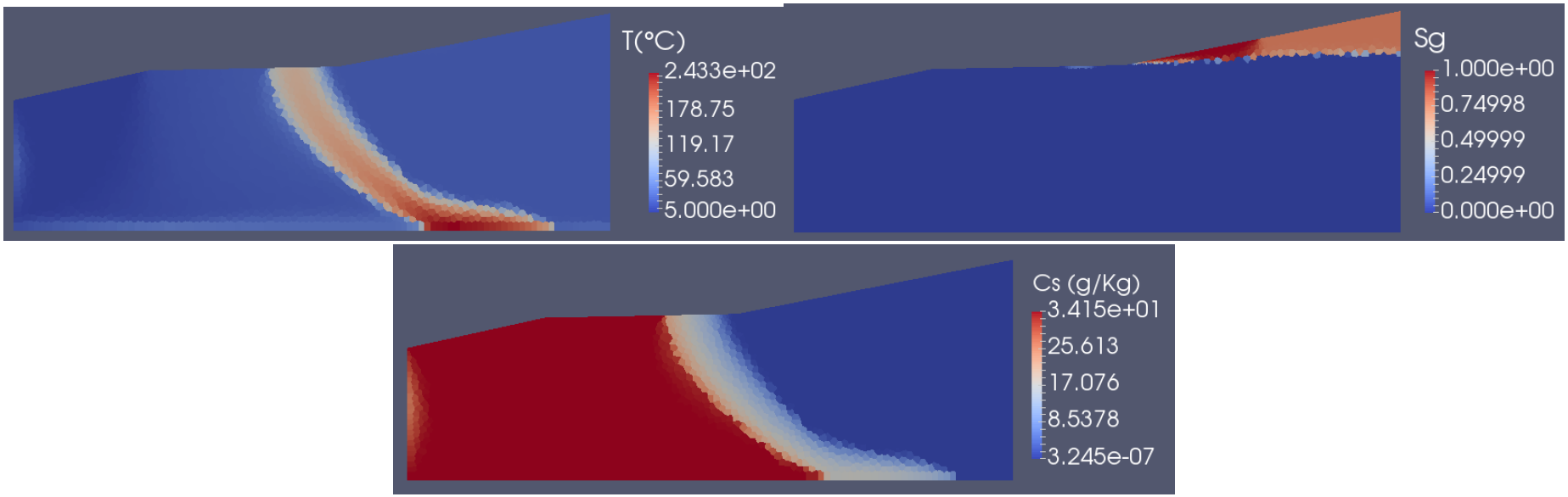

Figure: Temperature (in Celsius), gas saturation and salinity of the liquid phase (in $g.Kg^{-1}$) at final time (1000 years) obtained with the air-water-salt test case.

The sea water intrusion prevents the development of the convective thermal instabilities, this is due to the higher salinity of the sea water compared with the left side and bottom salinity. It also explains why the high temperature zone is shifted to the right.

Results: numerical impact of the advanced boundary condition

	Dirichlet	Atmospheric BC
Basic Newton-min	1002/98/6124/2041	×
Newton-min with projection	632/6/2788/944	699/25/3850/1334
Newton-min with projection and thermodynamic equilibrium	623/9/2779/920	646/13/3368/1137

Table: Number of time steps, of time step chops, total number of Newton iterations and CPU time obtained for the different versions of the Newton-min algorithm with the Dirichlet and the atmospheric top boundary condition.

Results: numerical impact of the salt

	3 comp. Atmospheric BC
Basic Newton-min	$\times$
Newton-min with projection	734/36/4204/2063
Newton-min with projection and thermodynamic equilibrium	626/31/3808/1863

Table: Number of time steps, of time step chops, total number of Newton iterations and CPU time obtained with the different versions of the Newton-min algorithm for the air-water-salt test case.

Basic Newton-min algorithm often fails to converge, enforcing the complementary constraints to hold at each Newton iterate considerably improves the convergence, the thermodynamic equilibrium update also improves a little the non-linear convergence.

Bilan

- Formulation and model of an soil-atmosphere boundary condition able to capture the evaporation and if necessary the liquid outflow.
- The evaporation-outflow boundary condition has a non-negligible impact on the geothermal simulation. Moreover, it is more difficult to set the Dirichlet constants than the physical constant of the advanced boundary condition.
- Newton-min convergence: necessity at least to project on the complementary constraints.

Layout

Perspectives

- *In progress:* TPFA - VAG (Vertex Approximate Gradient scheme) combined scheme,
- extension to a 3D domain with faults,
- parallelism of the model in the COMPASS code.

Questions ?